Ternary Alloy Electrocatalysts for Oxygen Reduction Reaction

Jin Luo[1], Lefu Yang[1,2], Binghui Chen[2], Chuanjian Zhong[1*]

(1. *Department of Chemistry, State University of New York at Binghamton, Binghamton, New York* 13902, *USA;*

2. *College of Chemistry and Chemical Engineering, Xiamen University, Xiamen* 361005, *Fujian, China*)

Abstract: Proton exchange membrane fuel cell represents an important electrochemical energy conversion device with many attractive features in terms of efficiency of energy conversion and minimization of environmental pollution. However, the large overpotential for oxygen reduction reaction at the cathode and the low activity, poor durability and high cost of platinum-based catalysts in the fuel cells constitute a focal point of major barriers to the commercialization of fuel cells. The development of nanostructured catalysts shows promises to addresses some of the challenging problems. The ability to engineer the composition and nanostructure of nanoalloy catalysts is important for developing active, robust and low-cost catalysts for fuel cell applications. This article highlights some of the recent insights into the catalytic properties of ternary nanoalloy catalysts prepared by molecularly-engineered synthesis and thermochemically-controlled processing, focusing on oxygen reduction reaction in fuel cells. This approach has demonstrated the abilities to control size, composition, and nanoscale alloying of binary and ternary nanoalloys. A highly-active ternary nanoalloy catalyst consisting of platinum, nickel and cobalt that is supported on carbon (PtNiCo/C) will be discussed as an example, highlighting the importance of nanoscale tuning of structures and composition for the design of fuel cell catalysts. The mass activity of selected PtNiCo/C catalysts has been shown much higher electrocatalytic activity than those observed for their binary counterparts and commercial Pt/C catalysts. Selected examples will also be shown that the catalytic activity can be tuned by the ternary composition. The structural and synergistic properties of the ternary nanoalloy catalysts for the enhancement of the electrocatalytic activity will also be discussed.

Key words: ternary nanoalloys; nanocatalysts; electrocatalytic activity; oxygen reduction reaction; fuel cells

CLC Number: O646   **Document Code:** A

1 Introduction

For pro ton exchange membrane fuel cell (PEMFC), an electrochemical energy conversion device, the large overpotential for oxygen reduction reaction (ORR) at the cathode represents a loss of about 20% from the theoretical maximum efficiency. The low activity, poor durability and high cost of platinum-based catalysts in PEMFCs constitute a major barrier to the commercialization of fuel cells. It is the kinetic limitation of the oxygen reduction at cathode catalysts which causes a problem for fuel cells operating at low temperature (<100 ℃). The rate of breaking O=O bond to form water strongly depends on the degree of its interaction with adsorp-tion sites of the catalyst. Many studies focused on understanding the mechanism of oxygen reduction on Pt—Fe, Pt—Ni, and Pt—Co [1], including CO- or methanol-tolerant catalysts [2]. Bulk-melted PtBi, PtIn, and PtPb intermetallic phases [3] and Ru nanoparticles modified with Pt [4] showed some promises for fuel cell applications. The application of high throughput, combinatorial screening methods to screen a large number of catalysts using an optical fluorescence technique by detecting proton production on an array of catalyst inks with different compositions has been successfully demonstrated [5]. Individually addressable array electrodes have been also investigated for rapid screening [6-7]. The high

throughput combinatorial screening of catalysts is very useful for rapid screening[8]. There are many examples of Pt alloys with early transition metals such as Co, Ni, Fe, Cr, Mn, V, etc. as catalysts for ORR in PEMFCs[9-10]. Studies on single crystalline thin films revealed that the addition of an early transition metal to Pt could change the atomic scale structures (Pt-Pt bond distance and coordination number) and electronic structures of Pt[11-12]. The ORR catalytic activity of these alloys is also dependent on the type and concentration of the second metal in the subsurface atomic layers[13-14]. The enhanced electrocatalytic activity of various Pt-based alloy catalysts arises from a combination of physical or chemical properties, including reduction of Pt-Pt distance, modified affinity for adsorption of hydroxide groups, d-orbital vacancy, formation of Pt skin as a result of base metal dissolution, crystal faceting, degree of alloying or atomic ordering, etc. While there are a number of reports on the detailed structural correlation of the fuel cell performance of Pt-based alloy catalysts [15-18], a clear understanding of these physical or chemical properties is lacking, largely due to the lack of precise control of the nanoscale composition and structures.

The preparation of catalysts from Pt alloyed with different transition metals has been an important focus for the development of fuel cell catalysts [2,19-20]. In many cases, the preparation of catalysts has been mostly based on traditional methods such as co-precipitation or impregnation[21-26], which are often not adequate for controlling size and composition of the catalysts. In contrast to most existing methods, the study of nano-engineered multimetallic alloy catalysts[8,27-31] has the potential in creating a synergistic balance of activity and stability of the catalysts. We have developed a strategy for nano-engineering the size, shape, composition and structural properties of multimetallic nanoparticles (e.g., AuPt, PtNi, PtCo, PtVFe, PtNiFe, PtNiCo, PtIrCo, etc.) as active and stable electrocatalysts for ORR[32-40], with some catalysts (e.g., AuPt, PtVFe and PtNiFe) tested in PEMFCs[37-40], demonstrating remarkable

effectiveness of the synthesis and processing strategy [8,27-30,41]. In this article, findings from our recent studies of a highly-active ternary nanoalloy catalyst (PtNiCo) are discussed, along with a brief summary of different ternary nanoalloy catalysts, highlighting the importance of nanoscale tuning of structures and composition for the design of advanced catalysts.

2 Catalyst Preparation

Traditional approaches to preparing supported nanoparticle catalysts involve co-precipitation, deposition-precipitation, ion-exchange, impregnation, successive reduction and calcination, etc. These methods have been widely used for preparing noble metal catalysts on support materials[42]. While a variety of supported Pt-group binary or ternary catalysts have been prepared by traditional methods[10,42-46], the ability to control the size and composition is limited due to the propensity of aggregation of metals at the nanoscale. The understanding of whether the formation of alloy or phase-segregation in multimetallic nanoparticles is different from the bulk scale materials, and how the catalytic activity and stability are influenced by size, composition, and morphology could hold keys to the engineering of durable and active catalysts.

Our strategy to the preparation of nanoalloy catalysts focuses on molecularly-engineered synthesis and thermochemically-refined processing. This strategy involves a sequence of three steps: solution-phase synthesis of the alloy nanoparticles with molecular encapsulation, assembly of the encapsulated nanoparticles on support materials, and thermochemical treatment of the supported nanoparticles [47]. For example, the general synthesis of the ternary PtNiCo nanoparticles involved reduction reactions of three metal precursors, $Pt^{II}(acac)_2$, $Ni^{II}(acac)_2$, and $Co^{II}(acac)_2$, in controlled molar ratios [34], forming PtNiCo nanoparticles capped with a monolayer of oleylamine/oleic acid molecules. The composition of $Pt^0_{n1}Ni^0_{n2}Co^0_{n3}$ nanoparticles, where $n1$, $n2$ and $n3$ represent the atomic percentages of each metal, is controlled by the feeding ratio of the metal precursors. For the synthesis of other trimetal-

lic nanoparticles, similar method was used. By controlling the relative concentrations of metal precursors and capping agents such as oleylamine and oleic acid, the nanoparticles of different compositions were synthesized. Fig. 1 shows TEM images for a few samples from the as-synthesized PtNiCo, PtCo, and PtNi nanoparticles.

Many of the binary or ternary nanoparticles can be easily assembled on carbon support materials with controllable dispersion and mass loading. Thermochemical treatments of the carbon-supported nanoparticles typically involved removal of organic capping molecules and calcination of the alloy structure. The average particle sizes after the thermochemical treatment show some slight increase in comparison with that before the treatment depending on the loading and the temperature. Importantly, as evidenced by high resolution TEM-EDX data, the ternary compositions of the particles of different sizes are found to be largely identical, and practically the same as the bulk composition obtained by bulk elemental analysis[8].

3 Electrocatalytic Activity for ORR

3.1 Measurement of Electrocatalytic Activity

The electrochemically active area (ECA) of the catalyst is determined from the voltammetric charges for the adsorption of hydrogen on the Pt sites of the nanoalloy, which is expressed in terms of cm^2 per unit of Pt mass in the catalyst. The electrocatalytic activity of the catalyst for ORR can be de-

termined by two methods (Fig. 2). One involves rotating disk electrode (RDE) measurement in which convection is achieved by the electrode rotating movement. The thickness of the diffusion layer is determined by the convection and the diffusion rate which are dependent on the rotating speed. The diffusion limiting current is determined by the rate at which the reactant diffuses to the surface of the electrode. The current of ORR is dependent on the kinetic current (i_k) and diffusion limiting current (i_d)[48-49]:

$$\frac{1}{i} = \frac{1}{i_k} + \frac{1}{i_d}$$

The limiting diffusion current is

$$i_d = 0.2\, n_e F\, C_0 D_0^{2/3}\, \nu^{-1/6}\, \omega^{1/2} = B\, \omega^{1/2}$$

where n_e is the number of electrons transferred per mole in the ORR process, F is Faraday constant, C_0 is the concentration of O_2 dissolved, D_0 is the diffusion coefficient of O_2 in the electrolyte, v is the viscosity of solution, and B is a constant that includes all these parameters, which is called Levich constant. For 0.1 mol·L^{-1} HClO$_4$ electrolyte, the kinetic current is often extracted at 0.900 V vs. RHE [32-40]. The kinetic current is used to determine the mass activity (MA, current density per unit mass of Pt) and specific activity (SA, current density per unit area of Pt). To obtain the MA and SA, the kinetic current is usually extracted from the RDE without IR-drop correction[56]. It is therefore important to point out that any comparison without IR-drop correction[56]. It is therefore important to point out that any comparison of MA or SA data determined from RDE mea-
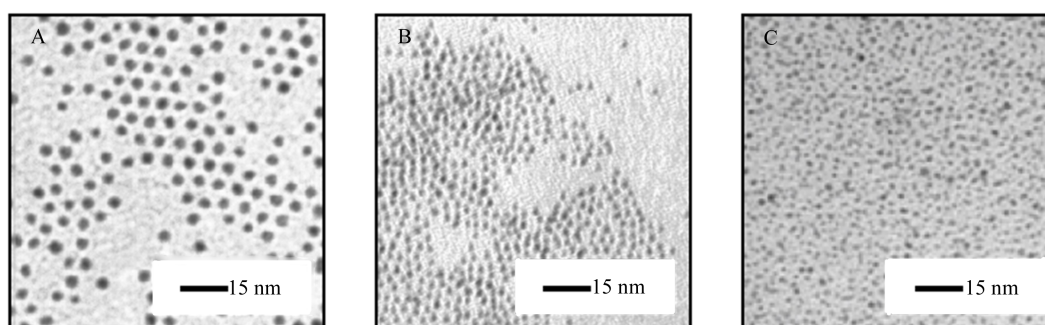

Fig. 1 TEM images for three samples of as-synthesized binary and ternary nanoparticles.
A. Pt$_{36}$Ni$_{15}$Co$_{49}$ (3.4 ± 0.4 nm); B. Pt$_{75}$Co$_{25}$ (1.8 ± 0.4 nm); C. Pt$_{78}$Ni$_{22}$ (1.5 ± 0.3 nm)
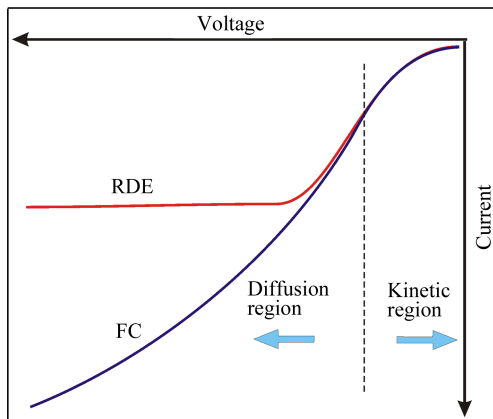
Fig. 2 A schematic illustration of the different regions of the *I-V* curves from measurement of membrane electrode assembly (MEA) in a fuel cell (FC) and from rotating disk electrode (RDE) in an electrochemical cell[57].

surements from different sources must consider the without *IR*-drop correction[56]. It is therefore important to point out that any comparison of MA or SA data determined from RDE measurements from different sources must consider the condition of data extraction.

Consider the RDE curve for a PtNiCo/C catalyst[34] to illustrate the difference of the mass/specific activity data between those obtained without and with *IR*-drop correction. The current in the kinetic region is shifted to a higher potential after the *IR* drop correction, from which the extracted mass activity is about 3 times higher than those reported for the same catalyst without *IR* correction[34]. In our work, all the mass activity data were determined from the kinetic region without the *IR* drop correction.

The second method involves determination of the polarization curve in a real fuel cell. A fuel cell (FC) system contains a membrane electrode assembly (MEA) consisting of catalyst layers and the proton exchange membrane. As illustrated in Fig. 2, the *I-V* curves coincide for the FC and RDE measurements at the kinetic region, but depart from each other in the diffusion region. The current extracted in the RDE at the kinetic region provides a good

measure of the electrocatalytic activity of the ORR electrocatalysts. Although the RDE measurement is often used to determine the electrocatalytic activity of catalysts, it does not provide a full picture on the electrocatalytic performance of the catalysts of MEA in a real fuel cell. Both RDE and MEA studies are sometimes required to fully characterize the catalyst activity and durability, providing important information on the performance of the catalysts from different perspectives.

The cell voltage is determined by the thermodynamic potential and the overpotential, $\eta_{\text{electrochemical process}}$, which includes both the anode and cathode overpotentials, i.e., $\eta_{\text{cathode}} - \eta_{\text{anode}}$, and the ohmic voltage η_{ohmic}, which can be summarized as,

$$E_{\text{cell}} = E_{\text{Nernst}} + \eta_{\text{electrochemical process}} - \eta_{\text{ohmic}} \quad (1)$$

where $\eta_{\text{electrochemical process}} = \eta_{\text{catalyst}} - \eta_{\text{conc.}}$. The total overvoltage associated with the $\eta_{\text{electrochemical process}}$ is dependent on the overpotentials associated with the catalyst activity (η_{catalyst}) and the concentration polarization ($\eta_{\text{conc.}}$). The activation overvoltage η_{catalyst} is mainly due to the sluggish activity of oxygen reduction reaction, whereas η_{conc} reflects a combination of reactant and product fluxes through the MEA, which is also a mass transfer overpotential. At the low current region, activation-related loss caused by the sluggish kinetics is the main reason for the drop of voltage, which includes the reactions, the catalysts and the reactant activities. With the current increasing, ohmic losses become more severe and lower the fuel cell performance. Ohmic loss is often caused by the internal ionic resistance in the fuel cell electrodes and electrolyte, electronic resistance of the electrodes and contact resistance. At the high current region, the limited diffusion of reactants to the reaction sites, i.e., the mass transport loss (concentration loss), decreases the fuel cell voltage. Characteristics from both RDE and MEA measurements are comparable in the kinetic region, but each measurement provides important information on the catalyst performance from different perspectives in terms of activity, stability, and other fuel cell param-

eters. In the kinetic region, the *I–V* curves also provides information for determining the activity of the catalyst.

3.2 Electrocatalytic Properties

The ternary PtNiCo catalyst is a recent example showing a major enhancement in electrocatalytic activity in comparison with its bimetallic counterparts[34,58]. Fig. 3 shows a representative set of cyclic voltammetry(CV) and RDE data for the $Pt_{36}Ni_{15}Co_{49}$/C catalysts treated at 400 (a), 700 (b), and 926 ℃ (c). In the kinetic region of the RDE curves at 0.900 V in 0.1 mol·L^{-1} HClO$_4$ electrolyte, there is a clear indication of the kinetic current increase with increasing the treatment temperature. The ECA value showed an initial gradual decrease as the temperature increased, but it remained constant for those with the treatment temperatures above 500 ℃. The

ECA decrease is apparently associated with the particle size increase. In Fig. 4A, the mass activity data was plotted as function of the thermal treatment temperature. There is a clear trend showing the increase of the mass activity with the treatment temperature. The mass activity of $Pt_{36}Ni_{15}Co_{49}$/C treated at 800 and 926 ℃ was more than 4 times higher than that of state-of-the-art Pt/C.

Both the specific activity and the lattice parameter have been found to depend on the thermal treatment temperature. There is a correlation between the specific activity and the lattice parameter (Fig. 4B). As the lattice shrinks as a result of the increased temperature treatment, the specific activity showed an increase. This increase occurred mostly for those with large lattice constants and those with small lattice constants. The change is relatively
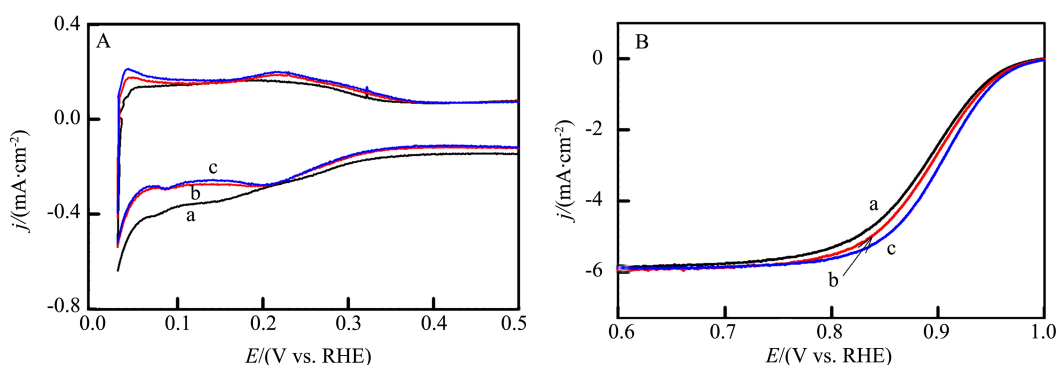
Fig. 3 CV (A) and RDE (B) curves for the PtNiCo/C catalysts treated at (a) 400 ℃, (b) 700 ℃, and (c) 926 ℃. Electrolyte: 0.1 mol·L^{-1} HClO$_4$. Pt loading = 6.6 μg·cm^{-2} on the electrode. Scan rate: 50 mV·s^{-1} (A) and 10 mV·s^{-1} (B). Rotating speed: 1600 r·min^{-1} (B)[34].
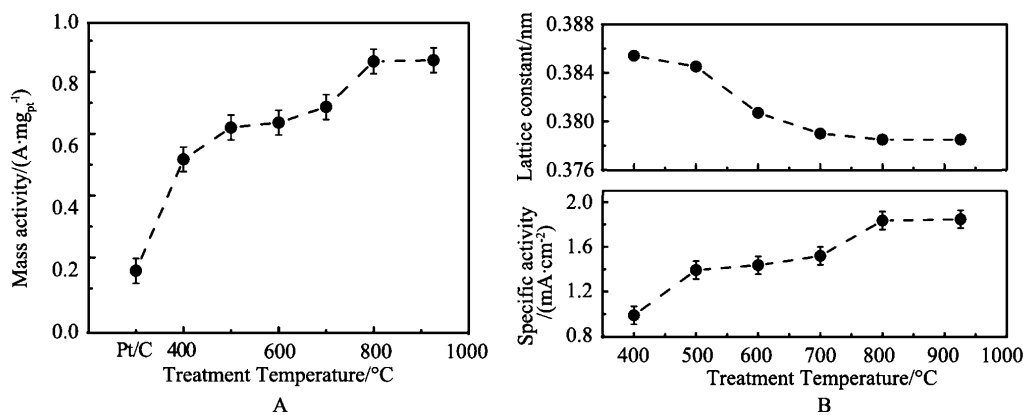
Fig. 4 A. Plots of mass activity for a set of $Pt_{36}Ni_{15}Co_{49}$/C catalysts treated at different temperatures. The result for a commercial Pt/C catalyst is included for comparison. B. Plots of specific activity and lattice parameter as a function of thermal treatment temperature[34].

small for the intermediate lattice constants. The lattice shrinking is believed to have played an important role in enhancing the electrocatalytic activity for catalysts treated at the higher temperatures. In addition, the electronic effect from the transition metal　(Co and Ni) in the subsurface may also enhance the activity of the Pt overlayer on the alloy surface. As suggested by the results of density functional theory　(DFT) computation, the d-band center of Pt overlayer on some relevant alloys formed either by the high temperature annealing or electrochemical dissolution of transition metals from the alloy surface shifted to a lower position with respect to the Fermi level due to compressive strain and electronic effect induced by the transition metals [59-60]. The downshifting of the d-band center results in a lower oxygen binding energy on the Pt overlayer. The oxygen binding energy on a pure Pt surface is too strong. A slightly weakening of it through alloying with other transition metals would lead to an increase in the activity. The ORR activity of PtNiCo catalysts thus strongly depends on the amount of compressive strain in the surface in addition to the electronic effect from the Co and Ni in the subsurface. Therefore, controlling the lattice constant of the alloys by adjusting the annealing temperature and the composition is an effective way to further tune the activity of Pt alloys.

The stability of the catalysts during potential cycling cab be examined by measurements after potential cycling of the catalysts between 0.02 V and 1.2 V, during which the transition metals on the catalyst surface may be leached out forming a Pt skin. As evidenced by the results, the increase in treatment temperature apparently increases the stability of the ECA value. In contrast, the mass activity for $Pt_{36}Ni_{15}Co_{49}$/C catalysts shows a significant reduction as a function of cycling numbers mostly after the initial 2000 cycles in comparison with that for Pt/C catalyst. Upon further cycling, the decrease of the mass activity is relatively small. The fast activity decay may be caused by the dissolution of transition metals in the alloys at high potentials.

One important strategy for tuning the catalytic activity involves thermochemical treatment of the catalysts under nitrogen　("minimum- or non-reactive" condition (MNC)) or oxygen (oxidative reaction condition (ORC)) atmosphere to produce different degree of oxidation, and subsequently under hydrogen atmosphere　(reductive reaction condition (RRC)) to reduce the oxidized components in the nanoparticles[58]　(Fig. 5A). This strategy has been demonstrated to impact the electrocatalytic activity of the PtNiCo catalysts in a significant way. For example, the catalyst is first heated at 260 ℃ in N_2 atmosphere for 30 min for the MNC treatment, or in
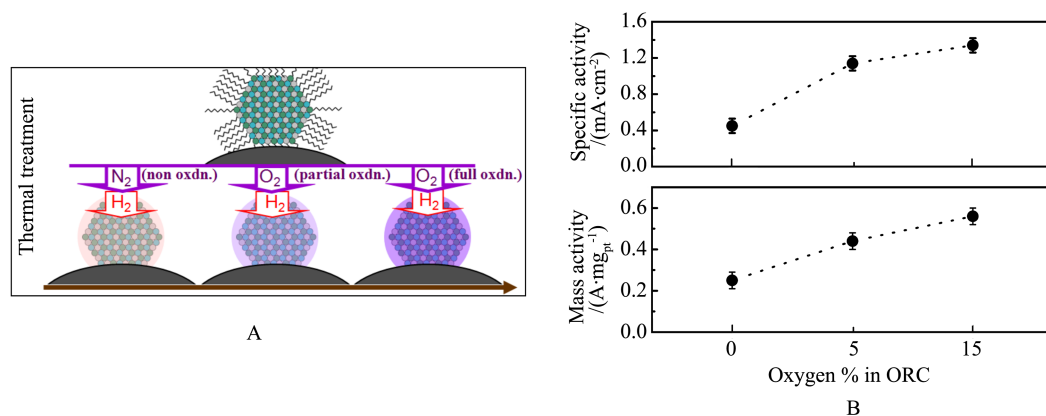

Fig. 5　A. An illustration of the thermochemical treatment of the catalyst under nitrogen　("minimum- or non-reactive" condition (MNC)) or oxygen (oxidative reaction condition (ORC)) atmosphere to produce different degree of oxidation, and subsequently under hydrogen atmosphere (reductive reaction condition (RRC)) to reduce the oxidized components in the nanoparticles. B. Comparison of mass and specific activities for $Pt_{39}Ni_{22}Co_{39}$/C catalysts treated under different O_2% in ORC: 0% (i.e., MNC-RRC), ORC (5% O_2, i.e., "LO")-RRC, and ORC (15%O_2, i.e., "HO")-RRC[58].

5% or 15% O_2 in an ORC treatment ("LO" or "HO"). The post ORC or MNC catalysts are then treated at 400 ℃ in 15% H_2 in an RRC treatment, i.e., ORC-RRC or MNC-RRC treatments. In Fig. 5B, the mass and specific activity data are plotted as a function of the oxygen concentration used in the ORC in the ORC-RRC treatments. There is a clear increase of the mass activity and the specific activity with the oxygen concentration in ORC. Note that the upper limit of the oxygen concentration in the ORC for the activity increase depends on the specific catalyst composition. By controlling the concentration of the oxygen in the thermal treatment, there is a clear increase in MA or SA by a factor of 2 ~ 3 from the MNC-RRC treated catalysts to the ORC-RRC treated catalysts.

The atomic-scale coordination structure of the catalysts has also been examined by EXAFS[58], revealing several important insights. First, the detected coordination numbers (CNs) for Pt-Ni from the catalysts treated by ORC ("LO")-RRC (Pt-Ni/Co, CN = 2.9) and ORC ("HO")-RRC (Pt-Ni/Co, CN = 4.5) are clearly indicative of the formation of Pt-Ni/Co alloy. There is also a reduction of Pt-Pt bond distance from 0.274 nm for ORC (Pt particle core) to 0.269 nm for ORC ("LO")-RRC and 0.268 nm for ORC ("HO")-RRC. The high oxygen content in the ORC results in a better alloying between Pt and Ni/Co upon the RRC treatment. In addition, there is a significant decrease in oxide content for the catalysts treated by ORC with a higher % O_2, which might have played a role in refining the alloy structure for the enhanced activity of the ORC ("HO")-RRC over ORC ("LO")-RRC or MNC-RRC catalysts (Fig. 5B).

Based on the results from an array of analytical characterizations, including TGA, TEM, XRD, EXAFS, and XPS, the differences in the observed catalytic activities are attributed to a combination of changes in the degree of alloying and the metal-metal and metal-oxygen coordination structures or catalysts subjected to these different thermochemical processing atmospheres[58]. This process is also ac-

companied by enrichment of Pt on the surface at the expense of Ni or Co. The higher degree of alloying favors the reduction of the fcc-type Pt–Pt lattice distances, which together with the surface enriched Pt, enhances the activation of the molecular oxygen. The reduced propensity of surface oxidation favors the availability of surface sites for removing oxygenated species adsorbed on the Pt sites following the reduction of molecular oxygen. A combination of the increase in the alloying degree, the decrease in oxide content, and the enrichment of surface Pt for the catalysts treated by the oxidative-reductive thermal processing has been concluded to be responsible for the enhanced electrocatalytic activity.

The data for the ternary catalyst have also been compared with those from the bimetallic counterparts, i.e., PtNi and PtCo catalysts[35] for assessing the catalyst composition and size effects on the electrocatalytic activity. If the effect of the subtle differences in composition on the mass activity is assumed to be relatively less significant than the size effect which is supported by the experimental data, and the degree of base metal leaching from the surface is assumed to be similar for PtNi/C and PtCo/C, there appears to be a sharp contrast in terms of mass activity dependence on the particle size. While the mass activity shows a decrease with the increase in particle size for PtCo/C catalysts in the 3 to 8 nm range, it exhibits an increase with the particle size for the PtNi/C catalysts. Note that a similar trend is also observed for the specific activity for the PtNi/C catalysts, though it is less significant for the PtCo/C catalysts. It is interesting to note that this trend is different from the size dependence of mass activity reported recently for Pt_3Co/C catalysts prepared by a different method[61-62], which showed a maximum mass activity at 4.5 nm. In the previous work, the size dependence was believed to reflect a balance of the average coordination number and the surface Co-leaching of the catalysts, and the enhanced adsorption of oxygenated species on the smaller sized particles, and consequently the decrease of the ORR activity. In another study[63] of PtCo catalysts with a

larger amount of oxygenated species, the surface Co oxides or subsurface species were found to exhibit a relatively-high specific activity. Based on our XAS data, we believe that the smaller Pt—Pt bond distance for PtCo/C than for PtNi/C is partially responsible for the higher activity for PtCo/C. It is possible that the observed difference in size dependence of activity for these two bimetallic catalysts was in part due to the difference in the amount of surface oxygenated species between these two types of alloy nanoparticles, which could lead to the difference in electrocatalytic activity for ORR[35,63]. This assessment is supported by the XAFS-detected subtle differences in Pt-M (M= Ni, and Co) bond distance and Pt—O coordination numbers, reflecting the presence of segregated phases in the PtNi nanoparticles and an enhanced adsorption of oxygenated species on PtCo nanoparticles, respectively.

By comparing the ORR mass/specific activities of the ternary PtNiCo/C catalyst[34] with its binary counterparts (PtNi/C and PtCo/C)[35], the ternary alloy catalyst clearly outperforms the binary ones (Tab. 1). This finding demonstrates a synergistic role played by the ternary alloy composition in the engineering the nanoparticle and the surface structures, details of which are being probed using synchrotron x-ray techniques in our ongoing work.

It is also important to emphasize that a number of ternary catalysts have been demonstrated to function as highly-active ORR catalysts[34,40,64-65], including PtNiCo/C, PtNiFe/C, PtIrCo/C, and PtVFe/C (Tab. 2). In our latest work, another ternary catalyst (PtVCo/C) was also found to exhibit high electro-

Tab. 1 Comparison of ORR mass/specific activities at 0.900 V in 0.1 mol·L⁻¹ HClO₄ (Note that the mass/specific activity data were extracted directly from the RDE curves without *IR*-drop correction)[34-35].

Catalyst	Mass activity /(A·mg$_{Pt}^{-1}$)	Specific activity /(mA·cm⁻²)
PtNiCo/C	0.88	1.76
PtNi/C	0.15	0.46
PtCo/C	0.27	0.51

Tab. 2 Comparison of ORR mass/specific activities for several catalysts (Pt/C, PtNiCo/C, PtIrCo/C, PtVFe/C, and PtNiFe/C) at 0.900 V in 0.1 mol·L⁻¹ HClO₄(Note that mass/specific activity data were extracted directly from the RDE curves without *IR*-drop correction)[34,40,64-65].

Catalyst	Mass activity /(A·mg$_{Pt}^{-1}$)	Specific activity /(mA·cm⁻²)
Pt/C (E-Tek)	0.22	0.24
PtNiCo/C	0.88	1.76
PtIrCo/C	0.72	1.23
PtVFe/C*	0.37	0.82
PtNiFe/C	0.38	0.80

* MA/SA at 0.858 V in 0.5 mol·L⁻¹ H₂SO₄.

catalytic activity for ORR (MA: 0.99 A·mg$_{Pt}^{-1}$; SA: 1.52 mA·cm⁻²). The catalysts not only showed enhanced catalytic activity over Pt/C catalyst, but also showed clear dependence on the nature of the base metals alloyed into Pt-ternary nanoparticles.

Many of the ternary catalysts have also been tested in a real fuel cell with MEAs loaded with the catalysts (e.g., PtNiCo/C, PtNiFe/C, and PtVFe/C) under a loading of 0.4 mg$_{Pt}$·cm⁻²[37-40,66]. Both the cell voltage and the peak power density for the fuel cells with these ternary catalysts have been shown to be greater than those for the fuel cell with Pt/C catalyst under the same test conditions. Some of the catalysts have also showed indications of enhanced stability, demonstrating the viability of the catalysts for applications in real fuel cells.

While promising leads to practical applications for some of the nanoalloy catalysts have been obtained based on the results from testing their performance in single-cell proton exchange membrane fuel cell, there are a number of fundamental issues yet to be addressed. One of the issues concerns the stability of base metals in the nanoalloy catalysts under the harsh operation condition of a fuel cell, which could lead to dissolution of base metals on the surface and the formation of the so-called Pt skin on the nanoalloy surface. While there are many studies focusing on the Pt-skin effect, the existing data do not provide satisfactory explanations to all experi-

mental facts of alloy catalysts, especially for nanoalloy catalysts. The question of how the nanoalloy structure can be perfected by refined processing strategies for achieving both high activity and high stability, or controlled by de-alloying process in the electrolyte for achieving stabilized activity and stability is increasingly important, which poses challenges to future research and development in fuel cell technology. Studies using various *in-situ* X-ray or spectroscopic techniques to address this question, part of our ongoing investigation, will provide some useful information in this regard.

4　Summary

In summary, effective strategies have been developed to produce Pt-based ternary alloy nanoparticles that exhibit enhanced electrocatalytic activities for oxygen reduction reaction in fuel cells. The synergistic properties of the ternary nanoalloy have played an important role in outperforming their binary counterparts in terms of the electrocatalytic activity. Further understanding of the atomic-scale structural correlation of the electrocatalytic properties of a wide range of binary[67-68] and ternary[34,40,64-65,69] nanoalloy catalysts for different fuel cell reactions will provide important insights for the rationale design of advanced catalysts.

Acknowledgments

References:

[1] Brandon N P, Skinner S, Steele B C H. Recent advances in materials for fuel cells[J]. Annual Review of Materials Research, 2003, 33: 183-213.

[2] Adler S B. Factors governing oxygen reduction in solid oxide fuel cell cathodes[J]. Chemical Reviews, 2004, 104 (10): 4791-4843.

[3] Casado-Rivera E, Volpe D J, Alden L, et al. Electro-catalytic activity of ordered intermetallic phases for fuel cell applications[J]. Journal of The American Chemical Society, 2004, 126(12): 4043-4049.

[4] Sasaki K, Wang J X, Balasubramanian M, et al. Ultra-low platinum content fuel cell anode electrocatalyst with a long-term performance stability[J]. Electrochimica Acta, 2004, 49(22/23): 3873-3877.

[5] Mallouk T E, Smotkin E S. Combinatorial catalyst development methods[M]//Handbook of fuel cells-fundamentals, technology and application. Vielstich W, Lamm A, Gasteiger H A, Edt. Chichester: John Wiley & Sons, 2003.

[6] Liu R, Smotkin E S. Array membrane electrode assemblies for high throughput screening of direct methanol fuel cell anode catalysts[J]. Journal of Electroanalytical Chemistry, 2002, 535(1/2): 49-55.

[7] Strasser P, Fan Q, Devenney M, et al. High throughput experimental and theoretical predictive screening of materials—A comparative study of search strategies for new fuel cell anode catalysts[J]. Journal of Physical Chemistry B, 2003, 107(40): 11013-11021.

[8] He T, Kreidler E, Xiong L, et al. Alloy electrocatalysts: Combinatorial discovery and nanosynthesis[J]. Journal of The Electrochemical Society, 2006, 153 (9): A1637-A1643.

[9] Stamenkovic V R, Mun B S, Arenz M, et al. Trends in electrocatalysis on extended and nanoscale Pt-bimetallic alloy surfaces[J]. Nature Materials, 2007, 6(3): 241-247.

[10] Paulus U A, Wokaun A, Scherer G G, et al. Oxygen reduction on carbon-supported Pt-Ni and Pt-Co alloy catalysts[J]. Journal of Physical Chemistry B, 2002, 106(16): 4181-4191.

[11] Greeley J, Stephens I E L, Bondarenko A S, et al. Alloys of platinum and early transition metals as oxygen reduction electrocatalysts[J]. Nature Chemistry, 2009, 1(7): 552-556.

[12] Stamenkovic V R, Fowler B, Mun B S, et al. Improved oxygen reduction activity on $Pt_3Ni(111)$ via increased surface site availability[J]. Science, 2007, 315 (5811): 493-497.

[13] Stamenkovic V, Schmidt T J, Ross P N, et al. Surface composition effects in electrocatalysis: Kinetics of oxygen reduction on well-defined Pt_3Ni and Pt_3Co alloy surfaces[J]. Journal of Physical Chemistry B, 2002, 106(46): 11970-11979.

[14] Mukerjee S, Srinivasan S, Soriaga M P, et al. Role of structural and ekectronic-properties of Pt and Pt alloys on electrocatalysis of oxygen reduction—an *in-situ* XANES and EXAFS investigation[J]. Journal of The Electrochemical Society, 1995, 142(5): 1409-1422.

[15] Wei Z D, Feng Y C, Li L, et al. Electrochemically syn-

thesized Cu/Pt core-shell catalysts on a porous carbon electrode for polymer electrolyte membrane fuel cells [J]. Journal of Power Sources, 2008, 180(1): 84-91.

[16] Mani P, Srivastava R, Strasser P. Dealloyed binary PtM₃ (M = Cu, Co, Ni) and ternary PtNi₃M (M = Cu, Co, Fe, Cr) electrocatalysts for the oxygen reduction reaction: Performance in polymer electrolyte membrane fuel cells [J]. Journal of Power Sources, 2011, 196(2): 666-673.

[17] Seo A, Lee J, Han K, Kim H. Performance and stability of Pt-based ternary alloy catalysts for PEMFC[J]. Electrochimica Acta, 2006, 52(4): 1603-1611.

[18] Yu P, Pemberton M, Plasse P. PtCo/C cathode catalyst for improved durability in PEMFCs[J]. Journal of Power Sources, 2005, 144(1): 11-20.

[19] Rao C R K, Trivedi D C. Chemical and electrochemical depositions of platinum group metals and their applications[J]. Coordination Chemistry Reviews, 2005, 249 (5/6): 613-631.

[20] Russell A E, Rose A. X-ray absorption Spectroscopy of low temperature fuel cell catalysts [J]. Chemical Reviews, 2004, 104(10): 4613-4635.

[21] Bond G C, Thompson D T. Catalysis by gold[J]. Catalysis reviews—science and engineering, 1999, 41(3/4): 319-388.

[22] Campbell C T. The active site in nanopaticle gold catalysis[J]. Science, 2004, 306(5694): 234-235.

[23] Chen M S, Goodman D W. The structure of catalytically active gold on titania[J]. Science, 2004, 306 (5694): 252-255.

[24] Davis R J. All that glitters is not Au-0[J]. Science, 2003, 301(5635): 926-927.

[25] Haruta M, Date M. Advances in the catalysis of Au nanoparticles[J]. Applied Catalysis A-General, 2001, 222(1/2): 427-437.

[26] Rolison D R. Catalytic nanoarchitectures—The importance of nothing and the unimportance of periodicity[J]. Science, 2003, 299(5613): 1698-1701.

[27] Luo J, Njoki P, Lin Y, et al. Activity-composition correlation of AuPt alloy nanoparticle catalysts in electrocatalytic reduction of oxygen[J]. Electrochemistry Communications, 2006, 8: 581-587.

[28] Luo J, Njoki P, Lin Y, et al. Characterization of carbon-supported AuPt nanoparticles for electrocatalytic methanol oxidation reaction[J]. Langmuir, 2006, 22: 2892-2898.

[29] Luo J, Kariuki N, Han L, et al. Preparation and characterization of carbon-supported PtVFe electrocatalysts[J]. Electrochimica Acta, 2006, 51(23): 4821-4827.

[30] Luo J, Wang L Y, Mott D, et al. Ternary alloy nanoparticles with controllable sizes and composition and electrocatalytic activity[J]. Journal of Materials Chemistry, 2006, 16: 1665-1673.

[31] Wang L, Luo J, Schadt M J, et al. Thin film assemblies of molecularly-linked metal nanoparticles and multifunctional properties[J]. Langmuir, 2010, 26: 618-632.

[32] Wanjala B N, Luo J, Loukrakpam R, et al. Nanoscale alloying, phase-segregation, and core-shell evolution of gold-platinum nanoparticles and their electrocatalytic effect on oxygen reduction reaction[J]. Chemistry of Materials, 2010, 22: 4282-4294.

[33] Wanjala B N, Luo J, Fang B, et al. Gold-platinum nanoparticles: Alloying or phase segregation[J]. Journal of Materials Chemistry, 2011, 21: 4012- 4020.

[34] Wanjala B N, Loukrakpam R, Luo J, et al. Thermal treatment of PtNiCo electroatalysts: Effects of nanoscale strain and structure on activity and stability for oxygen reduction reaction[J]. Journal of Physical Chemistry C, 2010, 114: 17580-17590.

[35] Loukrakpam R, Luo J, He T, et al. Nanoengineered Pt-Co and PtNi catalysts for oxygen reduction reaction: An assessment of the structural and electrocatalytic properties[J]. Journal of Physical Chemistry C, 2011, 115: 1682-1694.

[36] Loukrakpam R, Chang P, Luo J, et al. Chromium-assisted shape control of Pt-based nanoparticle electrocatalysts[J]. Chemical Communications, 2010, 46: 7184-7186.

[37] Fang B, Luo J, Chen Y, et al. Nanoengineered PtVFe/C cathode electrocatalysts in pem fuel cells: Catalyst activity and stability[J]. ChemCatChem, 2011, 3(3): 583-593.

[38] Fang B, Wanjala B N, Hu X A, et al. PEM Fuel Cells with nanoengineered AuPt catalysts at the cathode[J]. Journal of Power Sources, 2011, 196: 659-665.

[39] Fang B, Luo J, Njoki P N, et al. Nanoengineered PtVFe catalysts in proton exchange membrane fuel cells: Electrocatalytic performance[J]. Electrochimica Acta, 2010, 55: 8230-8236.

[40] Fang B, Luo J, Njoki P N, et al. Nanostructured PtVFe catalysts: Electrocatalytic performance in proton exchange membrane fuel cells [J]. Electrochemistry Communications, 2009, 11: 1139-1141.

[41] Luo J, Han L, Kariuki N N, et al. Phase properties of carbon-supported gold-platinum nanoparticles with different bimetallic compositions[J]. Chemistry of Materials, 2005, 17: 5282-5290.

[42] Klabunde K J. Nanoscale materials in chemistry[M].

New York: John Wiley & Sons, Inc., 2001.

[43] Feldheim D L, Foss Jr C A. Metal nanoparticles: Synthesis, characterization, and applications[M]. New York: Marcel Dekker, Inc., 2002.

[44] Raja R, Khimyak T, Thomas J M, et al. Single-step, highly active, and highly selective nanoparticle catalysts for the hydrogenation of key organic compounds [J]. Angewandte Chemie International Edition, 2001, 40 (24): 4638.

[45] Schmidt T J, Gasteiger H A, Behm R J. Methanol electrooxidation on a colloidal PtRu-alloy fuel-cell catalyst [J]. Electrochemistry Communications, 1999, 1(1): 1-4.

[46] Waszczuk P, Lu G Q, Wieckowski A, et al. UHV and electrochemical studies of CO and methanol adsorbed at platinum/ruthenium surfaces, and reference to fuel cell catalysis[J]. Electrochimica Acta, 2002, 47 (22/23): 3637-3652.

[47] Luo J, Fang B, Wanjala B N, et al. Nanoparticles for fuel cell applications[M]//Altavilla C, Ciliberto E, Edt. New York: Inorganic nanoparticles: Synthesis, applications, and perspectives. CRC Press, Taylor & Francis, 2010.

[48] Suarez-Alcantara K, Rodríguez-Castellanos A, Dante R, et al. $Ru_xCr_ySe_z$ electrocatalyst for oxygen reduction in a polymer electrolyte membrane fuel cell[J]. Journal of Power Sources, 2006, 157(1): 114-120.

[49] Guha A, Zawodzinski Jr T A, Schiraldi D A. Evaluation of electrochemical performance for surface-modified carbons as catalyst support in polymer electrolyte membrane (PEM) fuel cells[J]. Journal of Power Sources, 2007, 172(2): 530-541.

[50] Zhang J, Sasaki K, Sutter E, et al. Stabilization of platinum oxygen-reduction electrocatalysts using gold clusters[J]. Science, 2007, 315(5809): 220-222.

[51] Chen S, Gasteiger H A, Hayakawa K, et al. Platinum-alloy cathode catalyst degradation in proton exchange membrane fuel cells: Nanometer-scale compositional and morphological changes[J]. Journal of the Electrochemical Society, 2010, 157(1): A82-A97.

[52] Schulenburg H, Muller E, Khelashvili G, et al. Heat-treated $PtCo_3$ nanoparticles as oxygen reduction catalysts [J]. Journal of Physical Chemistry C, 2009, 113 (10): 4069-4077.

[53] Liu Z, Yu C, Rusakova I A., et al. Synthesis of Pt_3Co alloy nanocatalyst via reverse micelle for oxygen reduction reaction in PEMFCs[J]. Topics in Catalysis, 2008, 49(3/4): 241-250.

[54] Wang C, Chi M, Li D, Strmcnik D, et al. Design and synthesis of bimetallic electrocatalyst with multilayered Pt-skin surfaces[J]. Journal of the American Chemical Society, 2011, 133(36): 14396-14403.

[55] Wang C, van der Vliet D, Chang K C, et al. Monodisperse Pt_3Co nanoparticles as a catalyst for the oxygen reduction reaction: Size-dependent activity[J]. Journal of Physical Chemistry C, 2009, 113(45): 19365-19368.

[56] Van der Vliet D, Strmcnik D S, Wang C, et al. On the importance of correcting for the uncompensated Ohmic resistance in model experiments of the Oxygen Reduction Reaction[J]. Journal of Electroanalytical Chemistry, 2010, 647(1): 29-34.

[57] Zhong C J, Luo J, Fang B, et al. Nanostructured catalysts in fuel cells[J]. Nanotechnology, 2010, 21: 062001.

[58] Wanjala B N, Fang B, Loukrakpam R,et al. Role of metal coordination structures in enhancement of electrocatalytic activity of ternary nanoalloys for oxygen reduction reaction[J]. ACS Catalysis, 2012, 2(5): 795-806.

[59] Stamenkovic V, Mun B S, Mayrhofer K J J, et al. Changing the activity of electrocatalysts for oxygen reduction by tuning the surface electronic structure [J]. Angewandte Chemie International Edition, 2006, 45 (18): 2897-2901.

[60] Xu Y, Ruban A V, Mavrikakis M. Adsorption and dissociation of O_2 on Pt-Co and Pt-Fe alloys[J]. Journal of the American Chemical Society, 2004, 126(14): 4717-4725.

[61] Xu Q, Kreidler E, He T. Performance and durability of PtCo alloy catalysts for oxygen electroreduction in acidic environments[J]. Electrochimica Acta, 2010, 55 (26): 7551-7557.

[62] Wang C, Van der Vliet D, Chang K C, et al. Monodisperse Pt_3Co nanoparticles as electrocatalyst: the effects of particle size and pretreatment on electrocatalytic reduction of oxygen [J]. Physical Chemistry Chemical Physics, 2010, 12(26): 6933-6939.

[63] Koh S, Yu C, Mani P, et al. Activity of ordered and disordered Pt-Co alloy phases for the electroreduction of oxygen in catalysts with multiple coexisting phases[J]. Journal of Power Sources, 2007, 172(1): 50-56.

[64] Wanjala B, Fang B, Luo J, et al. Correlation between atomic coordination structure and enhanced electrocatalytic activity for trimetallic alloy catalysts[J]. Journal of the American Chemical Society, 2011, 133(32): 12714-12727.

[65] Loukrakpam R, Wanjala B N, Yin J, et al. Structural and electrocatalytic properties of nanoengineered PtIrCo catalysts for oxygen reduction reaction[J]. ACS Catalysis, 2011, 1(5): 562-572.

[66] Fang B, Wanjala B N, Yin J, et al. Electrocatalytic performance of Pt-based trimetallic nanoparticle catalysts in proton exchange membrane fuel cells[J]. International Journal of Hydrogen Energy, 2012, 37(5): 4627-4632.

[67] Chen G, You G, Zheng L, et al. Carbon-supported PtAu alloy nanoparticle catalysts for enhanced electrocatalytic oxidation of formic acid[J]. Journal of Power Sources, 2011, 196(20): 8323-8330.

[68] Chen G, Liao M, Li Y, et al. Pt-decorated PdAu/C nanocatalysts with ultralow Pt loading for formic acid electrooxidation[J]. International Journal of Hydrogen Energy, 2012, 37(130): 9959-9966.

[69] Wanjala B N, Fang B, Shan S, et al. Design of ternary nanoalloy catalysts: Effect of nanoscale alloying and structural perfection on electrocatalytic enhancement[J]. Chemistry of Materials, 2012, ASAP (dx.doi.org/10.1021/cm301613j).

三元合金氧还原电催化剂

罗　瑾[1], 杨乐夫[1,2], 陈秉辉[2], 钟传建[1*]

(1. 纽约州立大学宾汉姆顿分校化学系, 美国 纽约 13902;

2. 厦门大学化学化工学院, 福建 厦门 361005)

摘要: 质子交换膜燃料电池作为重要的电化学能源转换装置, 在提高能量转换效率、减少环境污染等方面具有诱人的前景. 然而, 阴极氧还原过电位较大、活性较低、稳定性差, 且铂基催化剂昂贵, 使该燃料电池难以商业化. 纳米结构电催化剂的发展有望解决此难题. 对纳米合金电催化剂其组分和结构的设计是开发高活性、高稳定性和低成本的燃料电池电催化剂的重要因素. 本文综述了近期由分子设计和热化学控制处理法制备的三元纳米合金电催化剂对燃料电池氧还原反应催化性能的最新进展. 该方法可控制纳米合金的尺寸、组成以及二元和三元纳米催化剂的合金化程度. 以高活性的三元纳米合金催化剂 PtNiCo/C 为例, 综述了在设计燃料电池电催化剂时结构和组成的纳米级调优的重要性. PtNiCo/C 电催化剂的质量比活性远高于其二元合金催化剂和 Pt/C 商业电催化剂. 三元电催化剂的催化活性可通过控制其组成来调节. 本文还讨论了三元纳米合金催化剂的结构及其协同效应对增强其电催化性能的影响.

关键词: 三元纳米合金; 纳米催化剂; 电催化活性; 氧还原反应; 燃料电池